Connecting point defect parameters with bulk properties to describe diffusion in solids

Chroneos, A

Original citation & hyperlink:
Chroneos, A 2016, 'Connecting point defect parameters with bulk properties to describe diffusion in solids' *Applied Physics Reviews*, vol 3, no. 4, 041304
https://dx.doi.org/10.1063/1.4968514

DOI 10.1063/1.4968514
ISSN 1931-9401

Publisher: AIP Publishing

Connecting point defect parameters with bulk properties to describe diffusion in solids

A. Chroneos

Citation: Appl. Phys. Rev. **3**, 041304 (2016); doi: 10.1063/1.4968514
View online: http://dx.doi.org/10.1063/1.4968514
View Table of Contents: http://aip.scitation.org/toc/are/3/4
Published by the American Institute of Physics

APPLIED PHYSICS REVIEWS

Connecting point defect parameters with bulk properties to describe diffusion in solids

A. Chroneos[1,2,a)]
[1]Department of Materials, Imperial College London, London SW7 2AZ, United Kingdom
[2]Faculty of Engineering, Environment and Computing, Coventry University, Priory Street, Coventry CV1 5FB, United Kingdom

(Received 12 August 2016; accepted 27 October 2016; published online 1 December 2016)

Diffusion is a fundamental process that can have an impact on numerous technological applications, such as nanoelectronics, nuclear materials, fuel cells, and batteries, whereas its understanding is important across scientific fields including materials science and geophysics. In numerous systems, it is difficult to experimentally determine the diffusion properties over a range of temperatures and pressures. This gap can be bridged by the use of thermodynamic models that link point defect parameters to bulk properties, which are more easily accessible. The present review offers a discussion on the applicability of the cBΩ model, which assumes that the defect Gibbs energy is proportional to the isothermal bulk modulus and the mean volume per atom. This thermodynamic model was first introduced 40 years ago; however, consequent advances in computational modelling and experimental techniques have regenerated the interest of the community in using it to calculate diffusion properties, particularly under extreme conditions. This work examines recent characteristic examples, in which the model has been employed in semiconductor and nuclear materials. Finally, there is a discussion on future directions and systems that will possibly be the focus of studies in the decades to come. *Published by AIP Publishing*. [http://dx.doi.org/10.1063/1.4968514]

TABLE OF CONTENTS

I. INTRODUCTION

The connection of point defect parameters with bulk properties in order to describe point defect properties in solids is a key issue in solid state physics.[1–20] In particular, nearly seventy years ago the Zener model[1,2] proposed that the Gibbs energy g^i (i = defect formation f, self diffusion activation act, or migration m) is proportional to the shear modulus of the solid and this provides physical insights considering the assumption that g^i accounts for the work to strain the lattice. Forty years ago, Varotsos *et al.*[3–6] proposed an alternative model refered to as the cBΩ model. This postulates that g^i is proportional to the isothermal bulk modulus B and the mean volume per atom Ω. Numerous studies have demonstrated the cBΩ model to be in better agreement with experimental studies than the Zener model (see Ref. 14 for review). Studies performed in the previous decades have established the efficacy of the cBΩ model in describing defect processes for numerous materials, including alkali and silver halides, PbF_2, AgI, nuclear fuels, gallium arsenide

a)Author to whom correspondence should be addressed. Electronic mail: alexander.chroneos@imperial.ac.uk

(GaAs), germanium (Ge), diamond, olivine, ZnO, LiH, silicon (Si), and others.[21–30]

The present review is mainly focused on the application of the cBΩ model and, in particular, on the interconnection between point defect parameters in solids and bulk properties. The focus is on calculating self- and dopant diffusion properties in systems where limited experimental data are available. The first part briefly introduces key point defect parameters and the important aspects concerning diffusion of the cBΩ model. The discussion then focuses on the applicability of the cBΩ model in describing diffusion properties in Ge, Si, and GaAs. The second part deals with the description of oxygen self-diffusion in nuclear fuels. This part is focussed on the ability of the cBΩ model to describe oxygen self-diffusion in uranium dioxide (UO_2) under pressure and oxygen self-diffusion in mixed-oxide (MOx) nuclear fuels. Finally, a brief summary and an outlook on future directions are offered in view of the recent advancements in computational modelling.

II. METHODOLOGY

A. Background of point defect parameters

The defect formation parameters of a crystalline material can be defined by comparing a real (i.e., defective) crystal to an isobaric ideal (i.e., non-defective) crystal.[11,14] The isobaric parameters are defined with respect to the corresponding Gibbs energy (g^f) as[11,14]

$$s^f = -\left.\frac{dg^f}{dT}\right|_P, \tag{1}$$

$$h^f = g^f - T\left.\frac{dg^f}{dT}\right|_P = g^f + Ts^f, \tag{2}$$

$$v^f = \left.\frac{dg^f}{dP}\right|_T, \tag{3}$$

where P is the pressure; T is the temperature; s^f, h^f, and v^f are the defect formation entropy, enthalpy, and volume, respectively.

In a crystalline material with a single diffusion mechanism, the self-diffusion process can be described by the activation Gibbs energy (g^{act}). The activation Gibbs energy is the sum of the Gibbs formation (g^f) and the Gibbs migration (g^m) processes. The activation entropy s^{act} and the activation enthalpy h^{act} are given by[11,14]

$$s^{act} = -\left.\frac{dg^{act}}{dT}\right|_P, \tag{4}$$

$$h^{act} = g^{act} + Ts^{act}. \tag{5}$$

The diffusion coefficient (or diffusivity) D is defined by

$$D = fa_0^2\nu e^{-\frac{g^{act}}{k_BT}}, \tag{6}$$

where f is the diffusion correlation factor, which depends upon the diffusion mechanism and the structure, a_0 is the lattice constant, ν is the attempt frequency, and k_B is Boltzmann's constant.

B. The cBΩ model

In the cBΩ model, the defect Gibbs energy g^i is related to the bulk modulus and the mean volume per atom of the solid via[3–9]

$$g^i = c^iB\Omega, \tag{7}$$

where c^i is dimensionless.

$$s^i = c^i\Omega\left(\beta B + \left.\frac{dB}{dT}\right|_P\right); \quad h^i = c^i\Omega\left(B - T\beta B - T\left.\frac{dB}{dT}\right|_P\right);$$
$$v^i = -c^i\Omega\left(\left.\frac{dB}{dP}\right|_T - 1\right), \tag{8}$$

where β is the thermal (volume) expansion coefficient.

A thermodynamic proof of the cBΩ model and the extent to which c can be considered as pressure and temperature independent is given by Varotsos and Alexopoulos (Chap. 14 of Ref. 11). In the bulk solid, one can prove the following relation:[11]

$$dG = \frac{d(BV)}{\left[(\partial B/\partial P)_T - 1\right]}. \tag{9}$$

When a solid is subjected to a small uniform deformation δ, the energy density u gained from this deformation is given by $u = \frac{1}{2}B\delta^2$. In this approximate scheme, B can be considered as a measure of the density of this elastic energy and hence "BV" is a measure of the total elastic energy stored in the body. Thus, Eq. (9) shows that in any isothermal process of a real (anharmonic) solid, the ratio of the variations of the "elastic energy BV" and the Gibbs energy G is equal to $\left(\frac{\partial B}{\partial P}\right)_T - 1$ (and not to -1, which would be valid if the solid were harmonic).

It can be also directly proven that the cBΩ formula $g^f = cB\Omega$ is just the relation

$$g^f = Bv^f/[(\partial B/\partial P)_T - 1] \tag{10}$$

with $c \equiv \left(\frac{v^f}{\Omega}\right)\Big/\left[\left(\frac{\partial B}{\partial P}\right)_T - 1\right]$. Equation (10) is strikingly similar to Eq. (9) which is valid for the macroscopic body.

In principle, when using the cBΩ model, the diffusion coefficient at any temperature and pressure can be calculated by means of a single experimental measurement. Combining Eqs. (6) and (7)

$$D = fa_0^2\nu e^{-\frac{c^{act}B\Omega}{k_BT}}. \tag{11}$$

Considering an experimentally determined diffusivity D_1 value at T_1, the c^{act} can be calculated, since the pre-exponential factor $fa_0^2\nu$ is either known or can be approximated. Then, using the value of c^{act}, the diffusivity D_2 at a temperature T_2 can be calculated employing Eq. (11),

provided that the elastic data and expansivity are known for this temperature. Commonly, c^{act} is regarded as a constant that can be assumed to be temperature and pressure independent to a first approximation.[11,14] Furthermore, s^{act}, h^{act}, and v^{act} can be calculated at any T using c^{act} in Eqs. (8)–(10). Finally, for constant T, the D can be studied at any pressure.

III. APPLICATIONS IN SEMICONDUCTORS

A. Self-diffusion in Si

1. Background

Si is traditionally the most important and investigated group IV semiconductor with numerous applications in microelectronic, sensor, and photovoltaic devices.[31–36] Key advances in the diffusion properties of group IV semiconductors are due to recent advances in experimental techniques (for example: Time-of-Flight Secondary Ions Mass Spectrometry, TOF-SIMS) and theoretical methods (such as density functional theory).[37–39] Intrinsic point defects (i.e., vacancies (V) and self-interstitials (I)) are the vehicles for self- and dopant diffusion in most crystalline materials including group IV semiconductors, such as Si and Ge.[37–39] Self-diffusion studies provide a direct route to intrinsic defect processes and therefore contribute to the understanding and control of diffusion during device fabrication.

2. Evidence of a single self-diffusion mechanism?

In a recent study, Saltas *et al.*[40] employed the cBΩ model to investigate the temperature dependence of self-diffusion in Si and the influence of the non-linear behavior of its bulk modulus at high temperatures to the point defect thermodynamic parameters. The experimental studies of Bracht *et al.*[41–43] covered a wide temperature range (923 K–1661 K) and revealed that the Arrhenius plot of self-diffusion in Si is curved (refer to Fig. 4 in Ref. 43). This, in turn, may imply that self-diffusion in Si cannot be described with a single diffusion mechanism.

In the study of Saltas *et al.*,[40] the mean volume per atom, $\Omega(T)$, was calculated from the lattice parameter, $a(T)$, given by

$$a(T) = a_o\left(1 + \int_{T_o}^{T} \alpha(T)dT\right), \tag{12}$$

where $a_o = 5.431$ Å is the lattice parameter at room temperature T_o. The linear thermal expansion coefficient over the temperature range 120 K–1500 K, $\alpha(T)$, is given by[44]

$$\alpha(T) = (3.725(1 - e^{-5.88\times10^{-3}(T-124)}) + 5.548 \times 10^{-4}T) \times 10^{-6}\,K^{-1}. \tag{13}$$

In Eq. (13), the isothermal bulk modulus $B(T)$ has been calculated from previous experimental data[45] of the adiabatic bulk modulus B_s, (temperature range 293 K–1273 K)

$$B(T) = \frac{B_s}{(1 + 3a\gamma T)}, \tag{14}$$

where a is given by Eq. (13) and the Grüneisen constant γ of Si is 0.367.[46]

Saltas *et al.*[40] used the 2nd order polynomial fitting describing B in the temperature range 873 K–1273 K to extrapolate the values of B at the higher temperature range (1273 K–1661 K, refer to Fig. 1). This is essentially based on the assumption that, in the higher temperature range B preserves the same functional relationship as T in the range 873 K to 1273 K.[40]

Figure 2 presents the experimental[41,42] self-diffusion coefficients of Si in the temperature range (923 K–1661 K) plotted as a function of $1000/T$ (Arrhenius plot) and as a function of $B\Omega/k_B$. It is important to note that the upward curved Arrhenius plot is converted into a straight line (with R-square = 0.99). The slope of this line is the c^{act} parameter of the cBΩ model (refer to Eq. (11)) and is equal to 0.311 ± 0.004.[40] It is therefore demonstrated (refer to Fig. 2) that there is no need to have both the V (at low temperature) and I (at high temperatures) self-diffusion mechanisms in Si, because the curved Arrhenius behavior can be accounted by the anharmonic behaviour of the bulk modulus.[40–42]

The study of Saltas *et al.*[40] concluded that the characteristic curved Arrhenius plot of self-diffusion in Si can be explained within the cBΩ thermodynamic model, using a single diffusion mechanism. The hypothesis in this study is the anharmonic behavior of the bulk modulus at high temperatures, which leads to temperature dependent activation properties.[40] This is consistent with the reported temperature-dependent activation enthalpy proposed for the contribution of V to Si self-diffusion.[40] The existence of a single self-diffusion mechanism in Si needs to be further investigated given that the prevailing picture is that both self-interstitials and vacancy mechanisms have an impact on self-diffusion in Si.

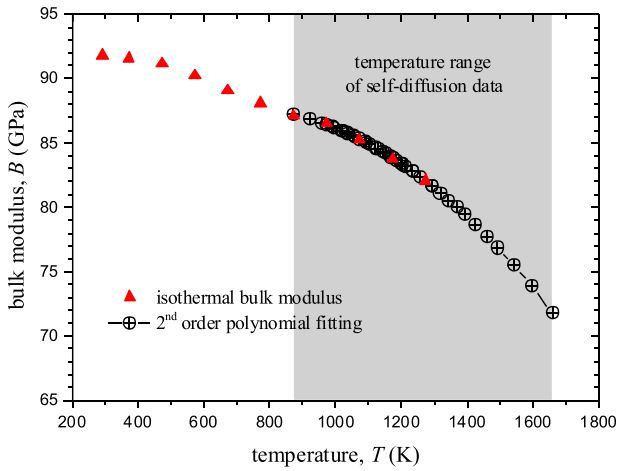

FIG. 1. The temperature dependence of the isothermal bulk modulus B that was derived from the experimentally determined of adiabatic bulk modulus B_S (temperature range 293 K–1273 K).[45] The grey shaded area highlights the range of the reported self-diffusion data.[41–43] For the higher temperatures, B values (where experimental self-diffusion data is available) were extrapolated, using 2nd order polynomial fitting in the range 873 K–1273 K. Reprinted with permission from Saltas *et al.*, Mater. Chem. Phys. **181**, 204 (2016). Copyright 2016 Elsevier.

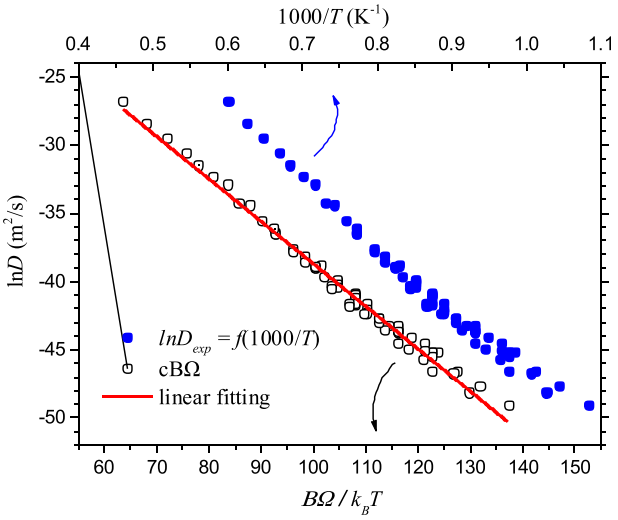

FIG. 2. The characteristic curved Arrhenius plot of the experimental self-diffusion coefficients in Si (blue circles).[42,43] The same data are plotted as a function of $B\Omega/k_BT$ (open circles), in the framework of the cBΩ model (Eq. (11)). The parameter c^{act} has been calculated by the fitted red line. Reprinted with permission from Saltas *et al.*, Mater. Chem. Phys. **181**, 204 (2016). Copyright 2016 Elsevier.

B. Diffusion in Ge

1. Self-diffusion

Although the defect processes of Ge have been studied since the early days of the microelectronics industry, the study of Werner *et al.*[47] determined the acceptor nature of the vacancy in Ge about thirty years ago. The vacancy self-diffusion mechanism in Ge was established given the agreement of Ge self-diffusion and the vacancy contribution to self-diffusion, derived from copper (Cu) diffusion in dislocation-free Ge.[48–50] More recently, Hüger *et al.*[51] observed that Ge self-diffusion in the temperature range 702 K–1177 K is described via the Arrhenius relation

$$D^V = 2.54e^{-\frac{3.13}{k_BT}} \times 10^{-3}\mathrm{m^2s^{-1}}. \quad (15)$$

The experimental data of Hüger *et al.*[51] show that, in this temperature range, the increase in diffusivity is about 9 orders of magnitude. Previous experimental data were used for expansivity and the isothermal bulk modulus.[52,53] The experimentally determined self-diffusion coefficients in Ge, with respect to $\frac{B\Omega}{k_BT}$, verified that the relation is linear and can be described by[30]

$$D^V_{cB\Omega} = 1.80e^{-\frac{-0.274B\Omega}{k_BT}} \times 10^{-5}\mathrm{m^2s^{-1}}. \quad (16)$$

The values derived by the cBΩ model are in excellent agreement with the experimental diffusion coefficients,[51] with differences being within 6%.[30]

The aforementioned agreement prompted Saltas and Vallianatos[29] to employ the cBΩ model to investigate the pressure dependence of self-diffusion coefficients in Ge. Experimentally, the impact of hydrostatic pressure (up to 600 MPa) and temperature on Ge self-diffusion had been reported by Werner *et al.*[47] Saltas and Vallianatos[29] calculated the diffusion coefficients with respect to P and T using the following relation:[11,19]

$$lnD(P,T) = lnD(0,T) - \left\{\frac{\upsilon^{act}(0,T)}{k_BT} - \kappa_o\gamma_o\right\}P + \left\{\frac{\kappa^{act}\upsilon^{act}(0,T)}{2k_BT}\right\}P^2, \quad (17)$$

where κ_o is the compressibility, γ_o is the Grüneisen constant, whereas $D(0,T)$ and $\upsilon^{act}(0,T)$ refer to zero pressure.[29] Additionally, κ^{act} is the compressibility of the activation volume[29]

$$\kappa^{act} = -\frac{1}{\upsilon^{act}}\left(\partial\upsilon^{act}/\partial P\right)_T. \quad (18)$$

This, in turn, can be expressed as a function of bulk properties using Eq. (10) as follows:[29]

$$\kappa^{act} = \kappa_o - \frac{\left(\partial^2B/\partial P^2\right)_T}{\left(\partial B/\partial P\right)_T - 1}. \quad (19)$$

It was previously determined that there is linear relationship for $B(P)$ over the pressure range 0–3 GPa. Therefore, $(\partial^2B/\partial P^2)_T$ is negligible and thus, $\kappa^{act} \approx \kappa_o$.[29,54] The values of Werner *et al.*[47] were used for $\kappa_o = 1.44 \times 10^{-11}Pa^{-1}$ and $\gamma_o = 0.72$. Using these parameters, υ^{act}, and the experimental diffusion coefficients at ambient pressure from Werner *et al.*[47] in Eq. (17), the diffusion coefficients can be calculated at any temperature and pressure.[29] Figure 3 shows the dependence of the $lnD(P,T)$ as a function of pressure at different temperatures in comparison to experimental values determined.[29,47] Figure 3 also demonstrates the good agreement between the cBΩ model and the experimental diffusion data for a range of pressures and temperatures. The calculations of Saltas and Vallianatos[29] are restricted to 3 GPa as there is a phase transition to Ge-II at this pressure and high temperatures.

2. Dopant diffusion

From an application viewpoint, the *n*-type dopants are the most important as the community pursued the formation

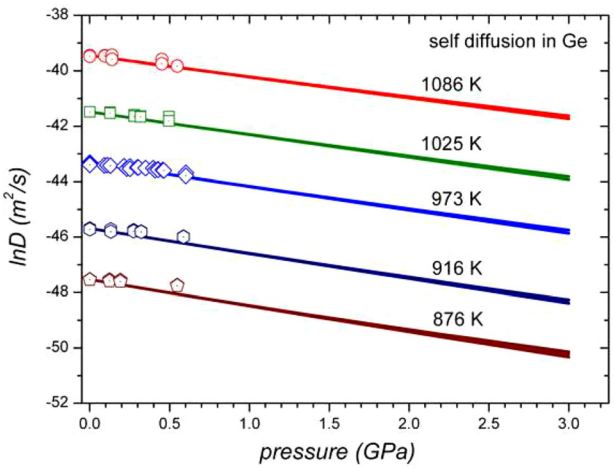

FIG. 3. The pressure dependence derived from the cBΩ model of Ge self-diffusion coefficients in germanium, at the temperature range 876 K–1086 K. The data points are the experimental values determined by Werner *et al.*[47] Reprinted with permission from V. Saltas and F. Vallianatos, Mater. Chem. Phys. **163**, 507 (2015). Copyright 2015 Elsevier.

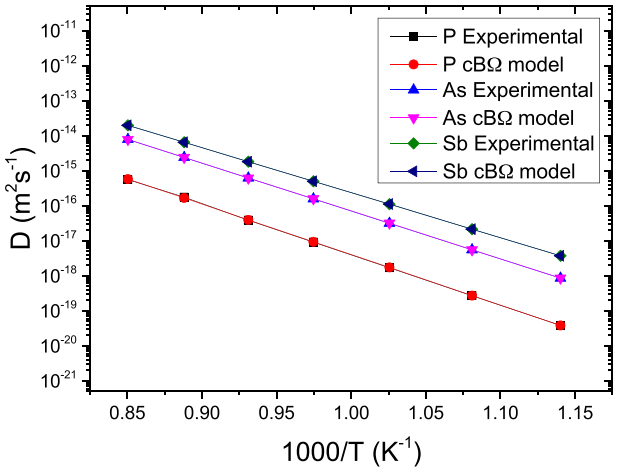

FIG. 4. Arrhenius plot for *n*-type dopant diffusion coefficients in Ge. A comparison of experimental results[56,57] and cBΩ model results.[30] Reprinted with permission from A. Chroneos and R. V. Vovk, Mater. Sci. Semicond. Process. **36**, 179 (2015). Copyright 2015 Elsevier.

of the *n*-MOSFET.[39,55] The technologically important *n*-type dopants (A) in Ge are phosphorous (P), arsenic (As), and antimony (Sb). Both experimental and theoretical studies agree that *n*-type dopants (P, As, and Sb) diffuse in Ge via vacancy-mediated mechanisms.[56–59] In particular, it was determined that the diffusion of *n*-type dopants increases with the square of the free electron concentration.[56,57] This behaviour can be accounted by considering singly negatively charged dopant-vacancy pairs, $(AV)^-$, formed by $(AV)^- \leftrightarrow A_s^+ + V^{2-}$ where A_s^+ is the singly positively charged *n*-type dopant and V^{2-} the doubly negatively charged vacancy.[56,57] It has been determined experimentally that the Ge *n*-type dopant diffusion can be described via Arrhenius relations (in the temperature range 873 K–1193 K)[56,57]

$$D_{exp}^{P} = 9.1e^{-\frac{2.85}{k_BT}} \times 10^{-4}\mathrm{m^2s^{-1}}, \quad (20)$$

$$D_{exp}^{As} = 3.2e^{-\frac{2.71}{k_BT}} \times 10^{-3}\mathrm{m^2s^{-1}}, \quad (21)$$

$$D_{exp}^{Sb} = 1.67e^{-\frac{2.55}{k_BT}} \times 10^{-3}\mathrm{m^2s^{-1}}. \quad (22)$$

A recent study demonstrated the validity of the cBΩ model in describing *n*-type dopant diffusion in Ge (refer to Fig. 4).[30] Equivalently to Eqs. (20)–(22), the Ge *n*-type dopant diffusion can be described in the framework of the cBΩ model via[30]

$$D_{cB\Omega}^{P} = 1.06e^{-\frac{0.25B\Omega}{k_BT}} \times 10^{-5}\mathrm{m^2s^{-1}}, \quad (23)$$

$$D_{cB\Omega}^{As} = 4.09e^{-\frac{0.2367B\Omega}{k_BT}} \times 10^{-5}\mathrm{m^2s^{-1}}, \quad (24)$$

$$D_{cB\Omega}^{Sb} = 2.77e^{-\frac{0.2228B\Omega}{k_BT}} \times 10^{-5}\mathrm{m^2s^{-1}}. \quad (25)$$

Other recent studies also employed the cBΩ model to describe dopant diffusion in Ge.[60–64] The results, which are summarized in Table I and compared to the available experimental results,[47,50,56,65–68] in essence provide a roadmap

TABLE I. Calculated values of the parameter c^{act}, activation enthalpy (h_{calc}^{act}), activation entropy (s^{act}), activation Gibbs free energy (g^{act}), and activation volume (v^{act}), in the framework of the cBΩ model for diffusion in Ge.[21,29,30,60–64] The results derived from the cBΩ model are compared to the available experimental results.[47,50,56,65–68] Error bars have been omitted for clarity.

Element	Temperature (K)	c^{act}	h_{calc}^{act} (eV)	h_{ecp}^{act} (eV)	s^{act} (k_B units)	g^{act} (eV)	v^{act} ($\times 10^{-29}$ m^3)
P	923–1193	0.239[a]	(2.57–2.74)[a]	2.85 ± 0.04[b]	(1.93–2.56)[a]	(2.39–2.56)[a]	1.09[a]
As	913–1193	0.227[a]	(2.45–2.61)[a]	2.71[b]	(1.83–2.45)[a]	(2.27–2.43)[a]	(1.03–1.04)[a]
Sb	873–1193	0.214[a]	(2.31–2.46)[a]	2.55[b]	(1.76–2.40)[a]	(2.14–2.29)[a]	0.98[a]
Al	827–1178	0.288[a]	(3.12–3.31)[a]	3.45[c]	(2.37–3.39)[a]	(2.90–3.07)[a]	1.32 ± 0.11[a]
Ge	808–1177	0.257[a]	(2.80–2.96)[a]	3.09[d]	(2.12–3.08)[a]	(2.59–2.75)[a]	(1.17–1.18)[a]
				3.14[e]			
Ge	850–1176	0.251[f]	…	…	12[a]	2.5[a]	…
Si	823–1173	0.278[a]	(3.01–3.20)[a]	3.32[h]	(2.30–3.28)[a]	(2.80–2.98)[a]	(1.27–1.28)[a]
		0.2909[g]					
In	827–1176	0.3078[i]	…	3.51[j]	…	…	…
Cu	827–1176	0.0158[k]	…	0.18[l]	…	…	…
Pd	827–1176	0.0026[m]	…	…	…	…	…
O	827–1176	−2.05[n]					

[a]Reference 29.
[b]Reference 56.
[c]Reference 65.
[d]Reference 47.
[e]Reference 66.
[f]Reference 21.
[g]Reference 61.
[h]Reference 67.
[i]Reference 60.
[j]Reference 68.
[k]Reference 62.
[l]Reference 50.
[m]Reference 63.
[n]Reference 64.

of all the parameters needed to model diffusion properties of the most technologically important dopants and impurities in Ge.

C. Dopant diffusion in GaAs

1. Background

Compared to Si, III–V semiconductors have advantageous material properties, including high electron mobility and—most importantly—the ability to lattice match with ternary (and/or quaternary) III–V compounds.[69–74] III–V materials have applications in nanoelectronic devices, radiation detectors, lasers, and solar cells.[75] GaAs is the archetypal III–V material that has been thoroughly investigated by the community for numerous years.[69–75] Previous studies have determined that Ga diffusion is the dominant self-diffusion mechanism in GaAs.[76] There are several investigations focusing on the diffusion of *n*- and *p*-type dopants in GaAs.[77–84] In GaAs, Si is a common *n*-type dopant when occupying the Ga Site (i.e., in As-rich growth conditions),[75] whereas Beryllium (Be) and Zinc (Zn) are the important *p*-type dopants.[79]

2. Thermodynamic parameters

Recently, Saltas *et al.*[85] employed the cBΩ thermodynamic model to study the thermodynamic parameters, self- and dopants diffusion in GaAs. Figure 5 represents the temperature dependence of point defect thermodynamic parameters in GaAs, within the framework of the cBΩ model.[85] It can be observed in Figure 5 that the calculated values of the activation Gibbs free energy decrease with temperature, whereas the corresponding term Ts^{act} increases.[85] The overall result is constant values of activation enthalpy, as $h^{act} = g^{act} + Ts^{act}$.[85] These calculated activation enthalpy values are in excellent agreement with the available experimental data (refer to Table I of Ref. 85).[76–78,86–88] The values of activation entropy were calculated by Saltas *et al.*[85]

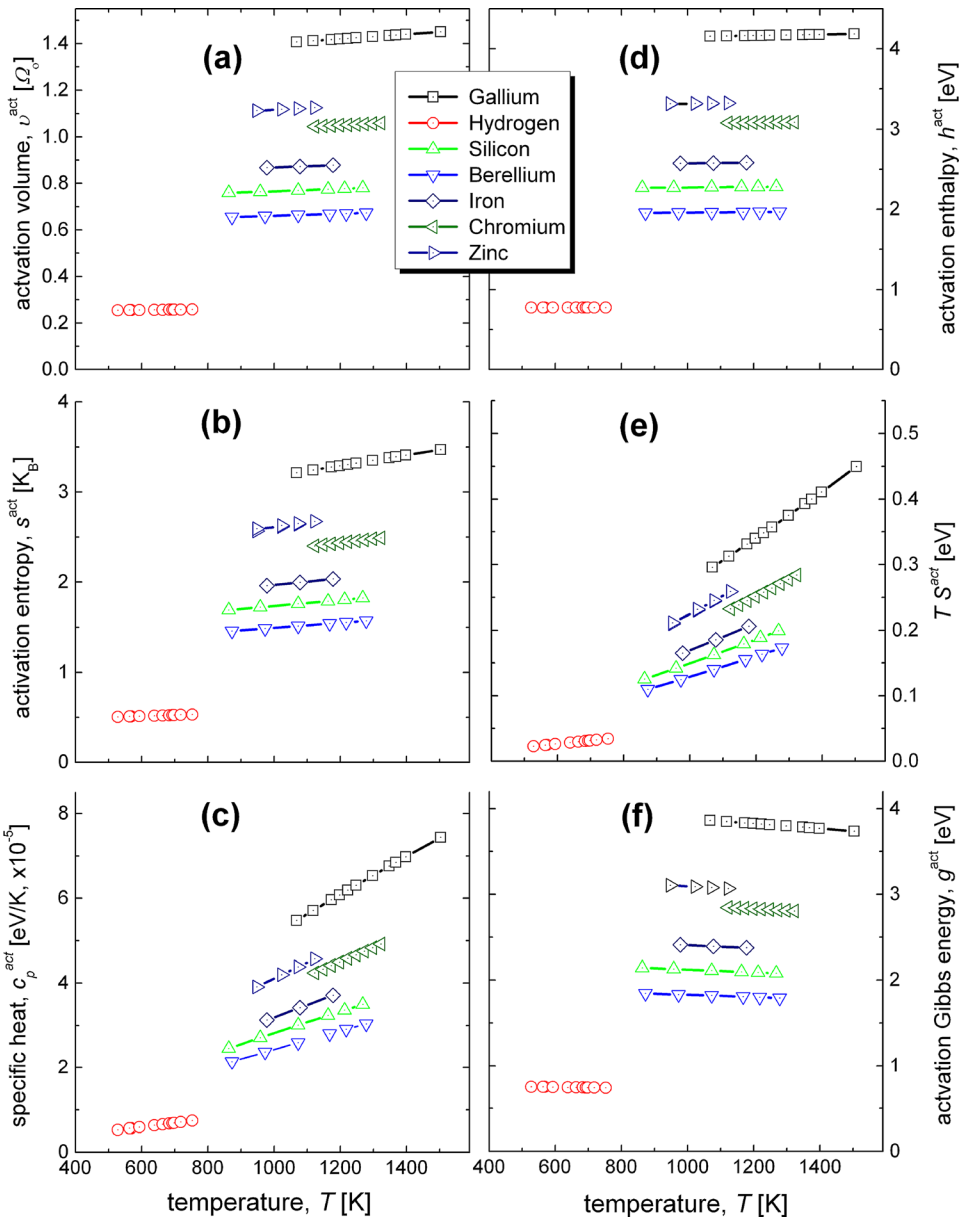

FIG. 5. The temperature dependence of point defect thermodynamic parameters [(a) Activation volume υ^{act}, (b) activation entropy s^{act}, (c) activation specific heat $c_P{}^{act}$, (d) activation enthalpy h^{act}, (e) the term Ts^{act} ($h^{act} = g^{act} + Ts^{act}$) and (e) the activation Gibbs free energy, g^{act}] of self- and dopant diffusion in GaAs, in the framework of the cBΩ model.[85] Reprinted with permission from Saltas *et al.*, RSC Adv. **6**, 53324 (2016). Copyright 2016 Royal Society of Chemistry.

using the cBΩ model, whereas the experimental activation entropies were calculated using

$$s_{exp}^{act} = k_B \ln\left(\frac{D_o}{gf\alpha^2\nu}\right), \tag{26}$$

where $g = 1$, $f = 1/2$, $\alpha = 5.653$ Å, and $\nu = 7.17 \times 10^{12}$ Hz.[76,78,85,89] There are errors in the activation entropy that appear due to the imprecise determination of activation enthalpy in diffusion experiments, the approximations in the values of f and g and the assumption that the attempt frequency is the Debye frequency.[85]

3. Pressure dependence of Ga self-diffusion

Saltas *et al.*[85] calculated the pressure dependence of Ga self-diffusion coefficients using the following relation that is valid for pressures up to 10 GPa, as at higher pressures GaAs transforms from zinc blende to orthorhombic:[90]

$$\ln D(P,T) = \ln D(0,T) - \left\{\frac{\upsilon^{act}(0,T)}{k_BT} - \kappa_o\left(\gamma_o - \frac{2}{3}\right)\right\}P + \left\{\frac{\kappa^{act}\upsilon^{act}(0,T)}{2k_BT}\right\}P^2 - \left\{\frac{(\kappa^{act})^2\upsilon^{act}(0,T)}{6k_BT}\right\}P^3, \tag{27}$$

where γ_o is the Grüneisen constant at zero pressure. The compressibility of the activation volume, κ^{act}, can be calculated by

$$\kappa^{act} = \kappa_o - \frac{(\partial^2 B/\partial P^2)_T}{(\partial B/\partial P)_T - 1}, \tag{28}$$

where $\kappa_o = 1/B_o$ and B_o is the bulk modulus at zero pressure, which is temperature dependent (refer to Fig. 1(c) of Ref. 85). Assuming that: $-B(\partial^2 B/\partial P^2)_T \approx (\partial B/\partial P)_T$,[91] κ^{act} is given by

$$\kappa^{act} \approx \kappa_o\left(1 + \frac{(\partial B/\partial P)_T}{(\partial B/\partial P)_T - 1}\right). \tag{29}$$

In the quasi-harmonic approximation, $(\partial B/\partial P)_T$ has a constant value that is pressure and temperature independent, whereas there is a slight variation upon compression in a real (anharmonic) solid.[11]

The Grüneisen constant can be calculated via the Dugdale-MacDonald equation[92]

$$\gamma = [(\partial B/\partial P)_T - 1]/2. \tag{30}$$

This has values in the range 1.80–1.84 for the temperature range (1068 K–1503 K).

Saltas *et al.*[85] used relations 27–30 to derive the pressure dependence of Ga self-diffusion coefficients in GaAs, as depicted in Fig. 6(a). Figure 6(b) represents the activation volume for Ga self-diffusion as a function of pressure and relies on the relation[85]

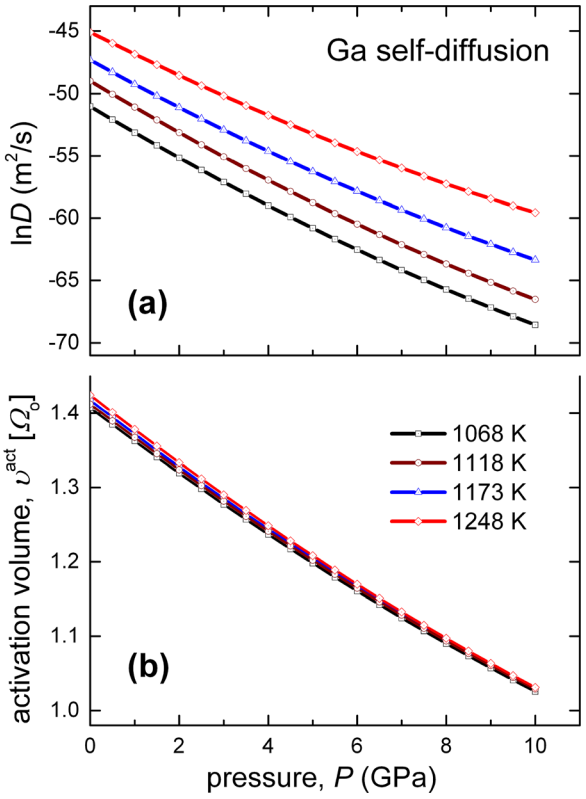

FIG. 6. (a) The cBΩ model derived pressure dependence of Ga self-diffusion coefficients in GaAsin, in the temperature range 1068–1248 K. (b) The corresponding variation of activation volumes.[85] Reprinted with permission from Saltas *et al.*, RSC Adv. **6**, 53324 (2016). Copyright 2016 Royal Society of Chemistry.

$$\upsilon^{act}(P,T) = \upsilon^{act}(0,T)\exp\left(-\int_0^P \kappa^{act}dP\right). \tag{31}$$

Fig. 6(b) also demonstrates that pressure has a more significant impact on the activation volume υ^{act} than temperature.[85]

4. Diffusion mechanisms of dopants

The detailed understanding of a diffusion process necessitates the determination of the activation energy, activation entropy, and activation volume.[93] Concerning the activation volume, the sign and magnitude can provide evidence on the diffusion mechanism. Saltas *et al.*[85] plotted the activation volume (at zero pressure) of dopants with respect to the atomic volume (refer to Fig. 7). The trend is that activation volume increases with the increase of the atomic volume of the dopants, with the exception of Ga and Fe.[85] H has a small activation volume ($\upsilon_H^{act} \approx 0.25\ \Omega_o$) and this is typical of a small atom that preferentially resides in interstitials positions.[85] For the larger Zn and Be diffusion in GaAs, $\upsilon_{Zn}^{act} > \upsilon_{Be}^{act}$ in the case of the larger Zn atom and this is consistent with diffusion in interstitial sites as opposed to vacancies where the contribution to the formation volume should be significant.[85] This in turn is consistent with the interstitial-substitutional mechanism (also known as the kick-out mechanism) that has been previously proposed for Zn and Be diffusion in GaAs by Yu *et al.*[79]

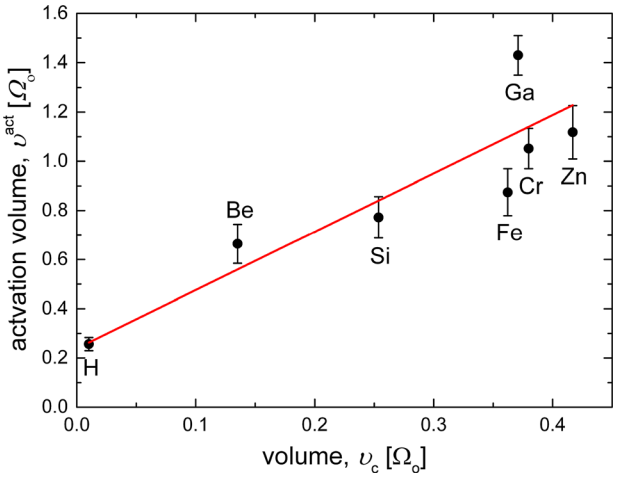

FIG. 7. Activation volume of dopants with respect to the atomic volume (derived from the covalent radius of the dopants). The (red) line is the linear fit of the data.[85] Reprinted with permission from Saltas *et al.*, RSC Adv. **6**, 53324 (2016). Copyright 2016 Royal Society of Chemistry.

IV. APPLICATIONS IN OXIDES

A. Background of nuclear fuels and methods

UO_2 is the principal component of conventional nuclear fuel and it can be blended with actinide oxides (for example, ThO_2 and PuO_2) to form mixed-oxide fuel.[94–97] The advantage of atomistic simulations is that they overcome the challenges of working with nuclear materials. This has been practiced by the community for decades and as a result there is now comprehensive data on nuclear fuel materials, which can be used to advance our understanding of their properties and/or complement experimental studies.[98–100]

MOx fuels are necessary for the sustainability of the nuclear industry and are applicable to alternative nuclear fuel cycles for traditional light-water reactors, as well as advanced fuels for the Generation IV reactors. Th is more abundant as compared to U.[96] Mixed Th and U based fuels have a high melting point and higher thermal conductivity compared to pure UO_2 fuels. Additionally, the U in $U_xTh_{1-x}O_2$ provides a source of fissile isotopes which are not present in pure ThO_2. Finally, the introduction of PuO_2, directly or as a MOx form, provides a way to take advantage of legacy stockpiles of the plutonium-rich material.

UO_2, ThO_2, and PuO_2, as well as their solid solutions, have a fluorite crystal structure. Understanding self-diffusion, and in particular, oxygen diffusion, in nuclear fuel is important in order to determine the physical properties of the fuel. In particular, oxygen diffusion in fuel is associated with the tolerance to radiation damage,[101] the accumulation of oxygen point defects into clusters (driving the formation of high burn up microstructures during operation),[102] and the solubility and migration of fission products.[103]

In recent studies, the cBΩ model was employed to investigate the defect processes in UO_2, PuO_2, ThO_2, and the mixed oxides.[26–28,104] An important difference between Section III, which considered semiconductor materials, and the work that will be described in oxides is that, in the latter, the material parameters upon which the model is based were not derived experimentally, but by using molecular dynamics. In particular, the Cooper-Rushton-Grimes (CRG) potentials derived by Cooper *et al.*[105] efficiently reproduce the thermomechanical and thermophysical properties of a range of related oxides (including AmO_2, CeO_2, CmO_2, NpO_2, PuO_2, ThO_2, and UO_2) for an extended temperature range. The efficacy of this approach lies on the CRG model introducing many-body interactions in the embedded atom method (EAM). The calculated elastic and diffusion properties in CeO_2, $U_{1-x}Th_xO_2$, and $Pu_{1-x}U_xO_2$ are in good agreement with the available experimental results.[105–109] Subsections IV B and IV C examine self-diffusion in UO_2 under pressure and describe self-diffusion in MOx nuclear fuels in the framework of the cBΩ model.

B. Self-diffusion in UO_2 under pressure

In a recent study, the cBΩ model was used to describe oxygen self-diffusion in UO_2 via the following relation:[27]

$$D_{cB\Omega}^{UO_2} = 1.277e^{-\frac{0.3052B\Omega}{k_BT}} \times 10^{-4}\mathrm{m^2s^{-1}}. \quad (32)$$

The expansivity and isothermal bulk modulus data were derived using MD within the CRG potential model for a range of temperatures and pressures.[28] In that study, the variation of bulk modulus as a function of pressure and temperature, B(T,P), was described by[28]

$$\mathrm{B(T,P)} = \mathrm{a} + \mathrm{b}\cdot\mathrm{T} + \mathrm{c}\cdot\mathrm{T}^2 + \mathrm{d}\cdot\mathrm{P} + \mathrm{e}\cdot\mathrm{P}^2 + \mathrm{f}\cdot\mathrm{P}\cdot\mathrm{T}, \quad (33)$$

where a is the bulk modulus at (T = 0, P = 0, i.e., 218 GPa), b (= -4.330×10^{-2} GPa K^{-1}) and c (= -1.846×10^{-6} GPa K^{-2}) represent temperature dependent terms, d (= 5.864) and e (= -1.387×10^{-1} GPa^{-1}) are dependent on pressure, and f (=1.301×10^{-3} K^{-1}) accounts for the interdependency between pressure and temperature.[28]

Figure 8 presents the pressure dependence for oxygen self-diffusion coefficients in UO_2 for the characteristic temperatures in the temperature range considered.[27] It is observed that hydrostatic pressure significantly reduces oxygen diffusivity in UO_2.[27] This is consistent with the impact of hydrostatic pressure on self-diffusion coefficients in other materials. For example, a similar trend was observed by Zhang and Wu[16] when they employed the cBΩ model to investigate self-diffusion in diamond under pressure.

An interesting consequence of hydrostatic pressure is that it affects the activation energies of oxygen diffusion (refer to Fig. 5 of Ref. 28). This dependence of the activation energy on pressure is given by[28]

$$\mathrm{E_a} = 5.66 + 0.123\cdot\mathrm{P}–0.00356\cdot\mathrm{P}^2. \quad (34)$$

It should be emphasised that, although the cBΩ model can be used to calculate oxygen self-diffusion (and other defect processes) in UO_2 over a range of pressures and temperatures, the model will not be applicable beyond the superionic transition temperature (note that the superionic transition marks the commencement of significant anion disorder in the lattice) because in this temperature a different c^{act} is required.[26,28] For example, Figure 9 illustrates, for the related PuO_2, the differences in the oxygen diffusivities in

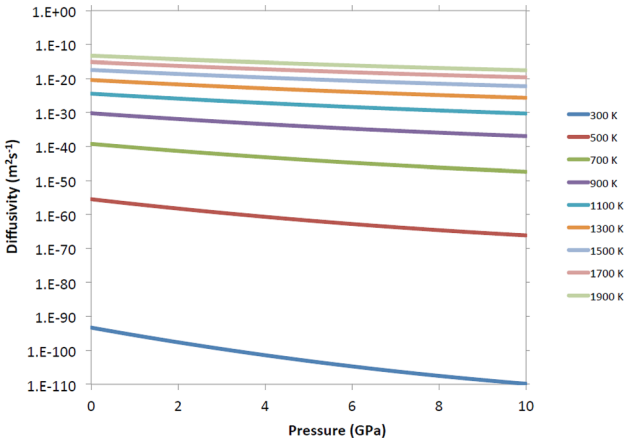

FIG. 8. Pressure dependence for oxygen self-diffusion coefficients in UO_2 derived by the cBΩ model for a wide temperature range (T = 300–1900 K).[28] Reprinted with permission from Cooper *et al.*, Solid State Ionics **282**, 26 (2015). Copyright 2015 Elsevier.

the superionic regime and the part where PuO_2 is fully crystalline.[26] Similarly, for hyperstoichiometric, UO_{2+x}, the cBΩ model is applicable but again with a different c^{act}. The efficacy of the cBΩ model in describing UO_2 for a wide range of P and T is what motivated the investigation of MOx nuclear fuels.[110]

C. Self-diffusion in MOx nuclear fuels

1. Framework of the Rose-Vinet equation of state

As it has been highlighted in the present review, it is essential for the cBΩ model to account for the pressure-volume-temperature data of the material. A way to do this is to use these data to fit in an equation of state. In the Rose-Vinet equation of state,[111] a material of volume, V, at an equilibrium temperature, T, and pressure, P, is interlinked via

$$P(T,X) = \frac{3B_0(T)}{X^2}(1 - X(V))\exp\left[\eta_0(T)(1 - X(V))\right], \quad (35)$$

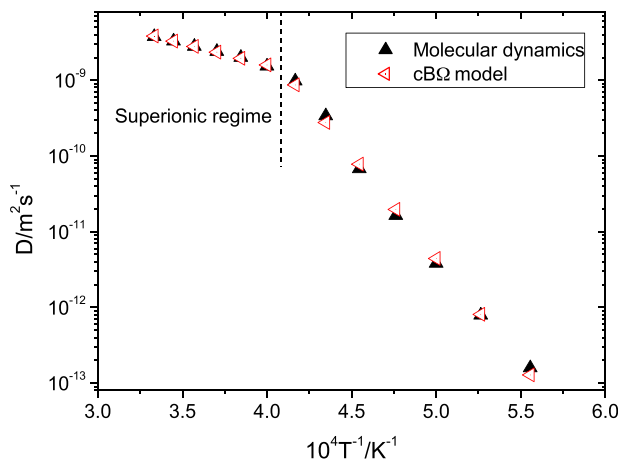

FIG. 9. The Arrhenius plot for oxygen diffusivity in PuO_2 calculated by MD[106] and derived by the cBΩ model.[26] The dashed line marks the range in which the superionic regime is applicable, up to the point where PuO_2 is fully crystalline.[26] Reprinted with permission from Chroneos *et al.*, J. Mater. Sci.: Mater. Electron. **26**, 3287 (2015). Copyright 2015 Springer.

where $B_0(T)$ is the zero pressure bulk modulus with respect to T and $X(V)$ the normalised length defined by

$$X(V) = \left[\frac{V}{V_0(T)}\right]^{1/3}, \quad (36)$$

where V is the material volume, $V_0(T)$ is the zero-pressure volume with respect to T, and $\eta_0(T)$ is given by

$$\eta_0(T) = \frac{3}{2}\left[\left.\frac{\partial B}{\partial P}\right|_0 (pT) - 1\right], \quad (37)$$

where $\frac{\partial B}{\partial P}|_0(T)$ is the pressure derivative of the bulk modulus at P = 0 as a function of T.

In the Rose-Vinet equation of state, the volume derivative of the Helmholtz free energy, $F(V,T)$, is divided into two terms[110]

$$P(V,T) = -\left(\frac{\partial F(T,V)}{\partial V}\right)_T = -\frac{dE(V)}{dV} + P_{them.}(T,V), \quad (38)$$

where $E(V)$ is the energy of the system at $T = 0$ K and $P_{\text{them.}}$ is a thermal pressure which tends to zero as $T \to 0$.[112,113] The pressure at a given volume and temperature is given by[110]

$$P(T,V) = P(T_R,V) + \alpha_0(T_R)B_0(T_R)(T - T_R). \quad (39)$$

In essence, $P(T,V)$ can be split into a term that has a dependence of the volume at reference temperature (T_R) and a term that is volume independent and linearly dependent upon T. Notably, Eq. (39) is valid above the material's Debye temperature (typically 300–400 K for MOx and when there are no phase transformations).[114,115]

According to Vinet *et al.*,[111] the pressure isotherm $P(T_R,V)$ at a non-zero temperature can be described by

$$H(T_R,X) \equiv \frac{X^2}{3(1-X)}P(T_R,X) = B_0(T_R)e^{\eta_0(T_R)(1-X)}, \quad (40)$$

where $H(T_R, X)$ is effectively motivated by Rose *et al.*[112] who investigated the scaling laws of the cohesive energy of materials with respect to their lattice parameter. Vinet *et al.*[111] obtained $B_0(T_R)$ and a gradient of $\eta_0(T_R)$ by the plot of $\ln(X)$ versus $(1-X)$.

An arbitrary reference temperature, T_R, is typically used to calculate the parameters for the Rose-Vinet equation of state.[110] The pressure isotherm $P(T_R, X)$ can be calculated using Eqs. (39) and (40)[110]

$$P(T,X_R) = \frac{3B_0(T_R)}{X_R^2}(1 - X_R)\exp\left[\eta_0(T_R)(1 - X_R)\right] + \alpha_0(T_R)B_0(T_R)(T - T_R). \quad (41)$$

The isothermal bulk modulus, $B(T,X_R)$, is given by[110]

$$B(T,X_R) = \frac{B_0(T_R)}{X_R^2}\left\{2 + [\eta_0(T_R) - 1]X_R - \eta_0(T_R)X_R^2\right\} \times \exp\left[\eta_0(T_R)(1 - X_R)\right] \quad (42)$$

and

$$\left[\frac{\partial B}{\partial P}\right](T,X_R) = \frac{4+[3\eta_0(T_R)-1]X_R+\eta_0(T_R)[\eta_0(T_R)-1]X_R^2-\eta_0^2(T_R)X_R^3}{3\left(2+[\eta_0(T_R)-1]X_R-\eta_0(T_R)X_R^2\right)}, \quad (43)$$

where $\alpha_0(T_R)$ is the zero pressure instantaneous thermal expansion at temperature T_R and X_R is given by Eq. (36) but evaluated at for $T=T_R$.

The Rose-Vinet equation of state is more complex than the more widely used isothermal Birch-Murnaghan equation of state.[116,117] Its main advantage though is that it can be used to calculate the volume of the material at an arbitrary T and P from only the thermal expansion coefficient, volume, bulk modulus, and pressure derivative of the bulk modulus at zero pressure and a *single* reference temperature T_R.[110]

The Levenberg–Marquardt least-squares algorithm[118,119] is an efficient way to fit $V_0(T_R)$, $B_0(T_R)$, $\frac{\partial B}{\partial P}|_0(T_R)$, and $\alpha_0(T_R)$ to the sets of P, V, and T data that are produced by the molecular dynamics simulations.[110] Thereafter, employing Eqs. (41)–(43) to predict volume, bulk modulus and the pressure derivative of the bulk modulus can be calculated.

In the study of Parfitt *et al.*,[110] the Rose-Vinet equation of state was fitted to the molecular dynamics data (within the CRG model) for the end members (i.e., UO_2, ThO_2, and PuO_2) and intermediate compositions ($U_xTh_{1-x}O_2$ and $U_xPu_{1-x}O_2$ for $x=0.25$, 0.5, and 0.75). In essence, the statistically averaged intermediate compositions and the consideration of V and T in the Rose-Vinet equation of state enable the calculation of the V at an arbitrary composition, pressure, and temperature.[110]

The bulk modulus of a solid solution $M_xN_{1-x}O_2$ is given by[110]

$$B(x) = B_N\frac{f(x)}{g(x)}, \quad (44)$$

where $f(x)$ and $g(x)$ are given by

$$f(x) = 1+x\left[\left(\frac{V_M}{V_N}\right)-1\right], \quad (45)$$

$$g(x) = 1+x\left[\left(\frac{B_NV_M}{B_MV_N}\right)-1\right], \quad (46)$$

where $B_{M,N}$ and $V_{M,N}$ are bulk moduli and equilibrium volumes of the end members MO_2 and NO_2. It has been shown (refer to Fig. 2 of Ref. 110) that the bulk modulus calculated from the relation above is in very good agreement with the values derived using the Rose-Vinet equation of state.

The pressure derivative of the bulk modulus with respect to the composition can calculated by Eq. (42)[110]

$$\frac{dB(x)}{dP} = B_N'\frac{f(x)}{g(x)}+B_N\frac{f'(x)g(x)-f(x)g'(x)}{g(x)^2}, \quad (47)$$

where $f'(x)$ and $g'(x)$ are the pressure derivatives of $f(x)$ and $g(x)$[110]

$$f'(x) = x\frac{V_M}{V_N}\left(\frac{1}{B_M}-\frac{1}{B_N}\right), \quad (48)$$

$$g'(x) = f'(x)+x\frac{V_MB_N}{V_NB_M}\left(\frac{B_N'}{B_N}-\frac{B_M'}{B_M}\right). \quad (49)$$

Again there is excellent agreement (refer to Fig. 2 of Ref. 110) and it can be deduced that the elastic properties at an arbitrary composition are well-represented by the relations considered above.

Finally, concerning the thermal expansivity, the variation in linear thermal expansion at zero pressure is defined as[110]

$$\frac{\Delta L(T)}{L(T_R)} = \frac{V(T)^{1/3}-V(T_R)^{1/3}}{V(T_R)^{1/3}}. \quad (50)$$

Parfitt *et al.*[110] calculated that the compositional variation is smaller for the PuO_2-UO_2 but greater for the ThO_2-UO_2 system. Additionally, the difference becomes greater at higher temperatures in agreement with previous experimental studies.[120]

2. Diffusion in MOx via the cBΩ model

Parfitt *et al.*[110] for simplicity made the assumption that a universal value of the pre-exponential holds irrespective of the composition and that only c_{act} can be allowed to vary depending on the composition of the oxide. This leads to the general expression

$$D_{cB\Omega}(M_xN_{1-x}O_2) = D_0e^{\frac{-C_{act}(x)B\Omega}{k_BT}}. \quad (51)$$

The activation coefficient with respect to the composition is given by[110]

$$c_{act}(x) = \sum_{n=0}^{N}a_nx^n. \quad (52)$$

Figure 10 represents the oxygen diffusivity (top part) and the dependence of the activation coefficient c_{act} with respect to the oxide composition in $U_xTh_{1-x}O_2$ and $U_xPu_{1-x}O_2$.[110] It is observed that c_{act} varies monotonically in the PuO_2-UO_2 system and increases as the Pu content is decreased.[110] For the ThO_2-UO_2 system, there is a minimum in c_{act} for x = 0.5 in agreement with the maximum in oxygen ion diffusivity from MD.

In essence, the study of Parfitt *et al.*[110] demonstrates how molecular dynamics simulations in synergy with thermodynamics models such as the cBΩ model can offer an understanding of the temperature and pressure dependent defect processes of energy related materials (Fig. 11). These methods can be employed to numerous systems where the defect and in particular, diffusion processes are difficult to determine.

V. SUMMARY AND FUTURE DIRECTIONS

A. Summary of models

To summarize, the association of point defect parameters to bulk properties is important because it positively

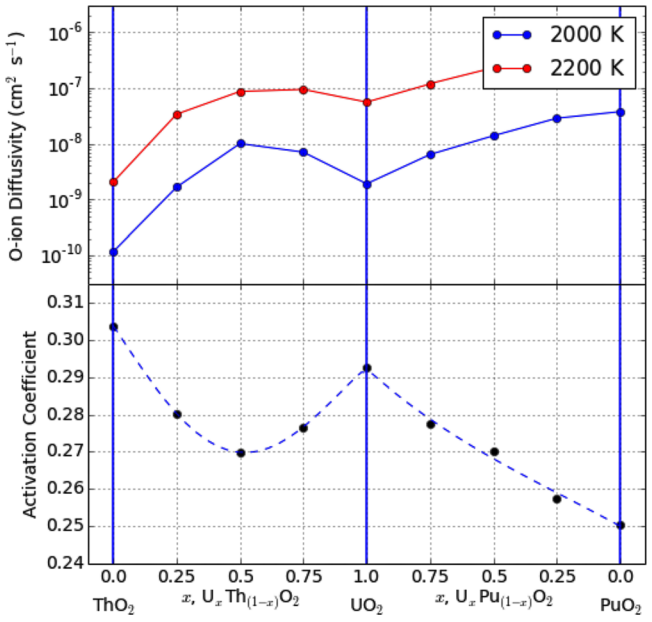

FIG. 10. The top part of the figure represents the oxygen diffusivity, whereas the bottom part represents the fitted values of the activation coefficient c_{act}, with respect to the oxide composition in the $U_xTh_{1-x}O_2$ and $U_xPu_{1-x}O_2$ systems. Dashed lines are the polynomial fits to the data for the $U_xTh_{1-x}O_2$ (forth-order polynomial) and the $U_xPu_{1-x}O_2$ (third-order polynomial).[110] Reprinted with permission from Parfitt *et al.*, RSC Adv. **6**, 74018 (2016). Copyright 2016 Royal Society of Chemistry.

affects the understanding of numerous technological issues, ranging from the optimization of nanoelectronic devices to the investigation of seismic phenomena.

The cBΩ model has been employed to describe the defect processes in solids for nearly forty years.[3–9] Most studies concern the derivation of defect parameters and in particular, diffusion coefficients, using a few data points of experimentally determined diffusion coefficients in conjunction with elastic and expansivity data for a range of temperatures. The method can be applicable even for a single diffusion coefficient if the pre-exponential factor is approximated.

In the present review, we discussed the applicability of the cBΩ model in MOx nuclear fuels, a system in which limited experimental data exist and systematic experiments are difficult to perform. This example was included to highlight the relevance of the cBΩ model in contemporary studies, where there are numerous advances in computational methods, power and resources compared to four decades ago. Modern computational methods facilitate the derivation of reliable defect parameters. However, problems remain in the calculation of diffusivities at low temperatures for systems in which the migration energy barriers are substantial. To exemplify the above, we provided a review of the study of Parfitt *et al.*,[110] where advanced MD calculations were employed in conjunction to the cBΩ model and the Rose-Vinet equation of state to calculate defect parameters in $Th_{1-x}U_xO_2$ or $Pu_{1-x}U_xO_2$. In essence, the model coefficients required to calculate self-diffusion coefficients at any pressure and temperature are: (a) volume, $V_0(T_R)$ (i.e., linear interpolation between end members), (b) bulk modulus $B_0(T_R)$, (c) pressure derivative of bulk Modulus, $\frac{\partial B}{\partial P}|_0(T_R)$, (d) thermal expansivity, $\alpha_0(T_R)$, and (e) the c_{act}.

In the decades to come, due to the constant increase in computational resources, it is anticipated that *ab initio* molecular dynamics of extended systems will become standard. At any rate, the cBΩ model will continue to be relevant in these *ab initio* molecular dynamics, since it can be employed in the same manner as the classical molecular dynamics calculations described above.

B. Conclusions and future directions

Concerning Si, in the study of Saltas *et al.*,[40] the cBΩ model revealed that the curved Arrhenius plot of self-diffusion can be explained by a single mechanism. The evidence

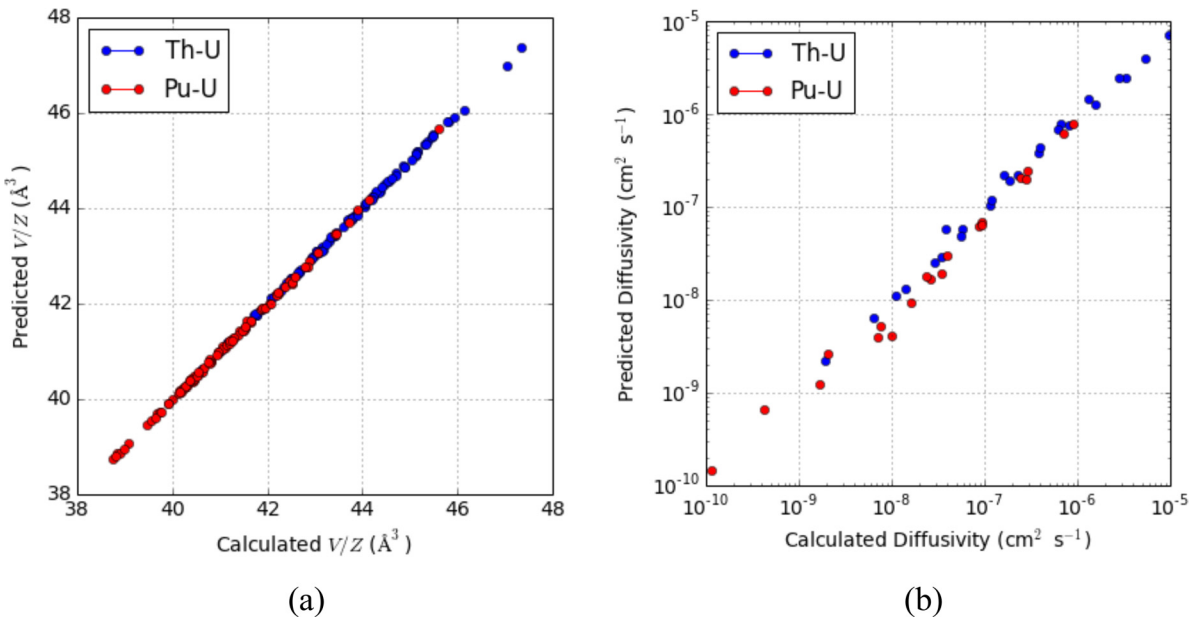

FIG. 11. cBΩ model and MD values of the (a) volume per formula unit and (b) oxygen diffusivity for a range of compositions.[110] Reprinted with permission from Parfitt *et al.*, RSC Adv. **6**, 74018 (2016). Copyright 2016 Royal Society of Chemistry.

provided for the single self-diffusion mechanism in Si is compelling but further experiments are required to test the accepted notion that there is a transition between interstitial and vacancy self-diffusion mechanisms at a certain temperature. This is because the transition may be hidden by the temperature dependence of the bulk properties. Additionally, further experimental data are required on the elastic properties in Si at high temperatures to verify the proposition of Saltas *et al.*[40] It should be noted that the non-linear behavior of the bulk modulus at high temperatures and the consequent curved Arrhenius plot has been linked in sodium (Na) and vanadium (V) to a single self-diffusion mechanism.[11,14] The elegance of the cBΩ thermodynamic model lies in the incorporation of the anharmonic elastic behavior of the solid to the calculation of its diffusion and other defect parameters. As there are numerous other curved Arrhenius plots, there are many materials that will need to be examined in order to reconsider the interpretation of the experimental diffusion data.

For Ge and GaAs, recent comprehensive studies using the cBΩ thermodynamic model have described defect processes including diffusion for most technologically important dopants.[29,30,60–64,85] For Ge, the pressure dependence of self-diffusion has been considered; however, future studies could investigate the pressure dependence of dopant diffusion. Although most of the issues concerning the cBΩ model in GaAs have been addressed for the most important dopants and impurities by Saltas *et al.*,[85] there is still ground to study other technologically important III–V compounds, such as GaSb and InSb. For example, previous experimental[121,122] and theoretical studies[123] have shown that self-diffusion in GaSb is asymmetric and that Ga diffuses more rapidly than Sb (up to three orders of magnitude). In this example, the cBΩ thermodynamic model could be employed to clarify the large disparity between the diffusion coefficients of the III and V elements.

The insights offered by the application of the cBΩ thermodynamic model in semiconductor materials could motivate systematic future investigations on the temperature and pressure dependence of defect process in ternary and quaternary semiconductor systems, where it is difficult to deconvolute the different contributions of the constituent components. For example, $Si_{1-x-y}Ge_xSn_y$ alloys are notable as they offer a range of strain options and they may be used to lattice match of Si or $Si_{1-x}Ge_x$ substrates with important III–V and II–VI compounds.[124–130]

Concerning the nuclear fuel oxides considered here, the stresses investigated are beyond those typically existing in a nuclear fuel pin. Nevertheless, they can be relevant when considering diffusion around microstructural defects (for example, the enhanced diffusion encountered near dislocation cores)[131,132] and in the modelling of oxide corrosion layers formed on metallic U, Pu, or Th.[110] This is because the latter are formed under significant compressive stresses due to the mismatch in the lattice parameter between the oxide and the metal.[110] The application of the cBΩ thermodynamic model can limit the use of expensive experiments and calculations (for example, in UO_2 the uranium ion *f*-electrons can complicate the identification of the ground state electronic structure.[133–135] The comprehensive study of the defect processes of MOx by Parfitt *et al.*[110] serves as an example for the application of the cBΩ model in conjunction to MD in oxides and materials. This methodology could lead to advances in energy materials (for example, materials for batteries and solid oxide fuel cells), where the requirement to optimize self-diffusion is limited by the complicated compositions and crystal structures of numerous materials.[136–140] Future work could include spinels and other geologically related materials, which present compositional complexity and high activation energies of diffusion.

ACKNOWLEDGMENTS

Co-authors of some of the papers reported here are acknowledged and, in particular, Professor Vasilis Saltas (TEI Crete), Dr. David Parfitt (Coventry University), and Dr. Michael Cooper (Los Alamos National Laboratory). The author is grateful for funding from the Lloyd's Register Foundation, a charitable foundation helping to protect life and property by supporting engineering-related education, public engagement and the application of research.

[1]C. Zener, J. Appl. Phys. **22**, 372 (1951).
[2]C. Wert and C. Zener, Phys. Rev. **76**, 1169 (1949).
[3]P. Varotsos and K. Alexopoulos, Phys. Rev. B **15**, 4111 (1977).
[4]P. Varotsos and K. Alexopoulos, Phys. Rev. B **15**, 2348 (1977).
[5]P. Varotsos and K. Alexopoulos, J. Phys. (Paris) Lett. **38**, L455 (1977).
[6]P. Varotsos, W. Ludwig, and K. Alexopoulos, Phys. Rev. B **18**, 2683 (1978).
[7]P. Varotsos and K. Alexopoulos, Phys. Rev. B **22**, 3130 (1980).
[8]P. Varotsos and K. Alexopoulos, Phys. Rev. B **24**, 904 (1981); K. Alexopoulos and P. Varotsos, *ibid.* **24**, 3606 (1981).
[9]P. Varotsos and K. Alexopoulos, Phys. Rev. B **30**, 7305 (1984).
[10]V. Saltas, A. Chroneos, M. W. D. Cooper, M. E. Fitzpatrick, and F. Vallianatos, RSC Adv. **6**, 103641 (2016).
[11]P. Varotsos and K. Alexopoulos, *Thermodynamics of Point Defects and their Relation with the Bulk Properties* (North-Holland, Amsterdam, 1986).
[12]P. Varotsos, N. Sarlis, and M. Lazaridou, Phys. Rev. B **59**, 24 (1999).
[13]P. Varotsos, Phys. Rev. B **75**, 172107 (2007).
[14]P. Varotsos, J. Appl. Phys. **101**, 123503 (2007).
[15]H. B. Su, D. O. Welch, W. Wong-Ng, L. P. Cook, and Z. Yang, Appl. Phys. Lett. **91**, 172510 (2007).
[16]B. H. Zhang and X. P. Wu, Appl. Phys. Lett. **100**, 051901 (2012); B. H. Zhang, C. Li, and S. Shan, Phys. Chem. Miner. **43**, 371 (2016).
[17]I. Sakellis, A. N. Papathanassiou, and J. Grammatikakis, Synth. Met. **161**, 2732 (2012); I. Sakellis, J. Appl. Phys. **112**, 013504 (2012).
[18]B. H. Zhang, AIP Adv. **4**, 017128 (2014).
[19]F. Vallianatos and V. Saltas, Phys. Chem. Miner. **41**, 181 (2014).
[20]E. S. Skordas, Solid State Ionics **195**, 43 (2011); E. S. Skordas, *ibid.* **261**, 26 (2014); E. S. Skordas, Mod. Phys. Lett. B **30**, 1650062 (2016); N. V. Sarlis and E. S. Skordas, J. Phys. Chem. A **120**, 1601 (2016); E. S. Skordas, Mater. Sci. Semicond. Proc. **43**, 65 (2016).
[21]V. Hadjicontis, K. Eftaxias, and P. Varotsos, Phys. Rev. B **37**, 4265 (1988); S.-R. G. Christopoulos, A. Kordatos, M. W. D. Cooper, and A. Chroneos, Mater. Res. Express **3**, 105504 (2016); V. Hadjicontis and K. Eftaxias, J. Phys. Chem. Solids **52**, 437 (1991); K. Eftaxias, V. Hadjicontis, and C. Varotsos, *ibid.* **52**, 523 (1991).
[22]B. H. Zhang, X. P. Wu, J. S. Xu, and R. L. Zhou, J. Appl. Phys. **108**, 053505 (2010); B. H. Zhang, X. P. Wu, and R. L. Zhou, Solid State Ionics **186**, 20 (2011).
[23]E. Ganniari-Papageorgiou, M. E. Fitzpatrick, and A. Chroneos, J. Mater. Sci.: Mater. Electron. **26**, 8421 (2015).
[24]P. Varotsos and K. Alexopoulos, Phys. Status Solidi B **110**, 9 (1982); M. Lazaridou, C. Varotsos, K. Alexopoulos, and P. Varotsos, J. Phys. C: Solid State **18**, 3891 (1985); P. Varotsos, Solid State Ionics **179**, 438 (2008).

[25]E. Dologlou, J. Appl. Phys. **110**, 036103 (2011); B. H. Zhang and X. P. Wu, Chin. Phys. B **22**, 056601 (2013).
[26]A. Chroneos, M. E. Fitzpatrick, and L. H. Tsoukalas, J. Mater. Sci.: Mater. Electron. **26**, 3287 (2015).
[27]A. Chroneos and R. V. Vovk, Solid State Ionics **274**, 1 (2015).
[28]M. W. D. Cooper, R. W. Grimes, M. E. Fitzpatrick, and A. Chroneos, Solid State Ionics **282**, 26 (2015).
[29]V. Saltas and F. Vallianatos, Mater. Chem. Phys. **163**, 507 (2015).
[30]A. Chroneos and R. V. Vovk, Mater. Sci. Semicond. Process. **36**, 179 (2015).
[31]S. Takeuchi, Y. Shimura, O. Nakatsuka, S. Zaima, M. Ogawa, and A. Sakai, Appl. Phys. Lett. **92**, 231916 (2008).
[32]A. Chroneos and H. Bracht, J. Appl. Phys. **104**, 076108 (2008); A. Chroneos, R. W. Grimes, and H. Bracht, *ibid.* **105**, 016102 (2009); A. Chroneos, C. A. Londos, and E. N. Sgourou, *ibid.* **110**, 093507 (2011); A. Chroneos, C. A. Londos, E. N. Sgourou, and P. Pochet, Appl. Phys. Lett. **99**, 241901 (2011).
[33]E. Kamiyama, K. Sueoka, and J. Vanhellemont, J. Appl. Phys. **111**, 083507 (2012).
[34]C. Gao, X. Ma, J. Zhao, and D. Yang, J. Appl. Phys. **113**, 093511 (2013); X. Zhu, X. Yu, and D. Yang, J. Cryst. Growth **401**, 141 (2014); P. Chen, X. Yu, X. Liu, X. Chen, Y. Wu, and D. Yang, Appl. Phys. Lett. **102**, 082107 (2013).
[35]C. A. Londos, Phys. Stat. Solidi A **102**, 639 (1987); C. A. Londos, M. S. Potsidi, and E. Stakakis, Physica B **340–342**, 551 (2003); A. Misiuk, J. Bak-Misiuk, A. Barez, A. Romano-Rodriguez, I. V. Antonova, V. P. Popov, C. A. Londos, and J. Jun, Inter. J. Hydrogen Energy **26**, 483 (2001); A. Chroneos, Phys. Status Solidi B **244**, 3206 (2007).
[36]A. Chroneos, E. N. Sgourou, C. A. Londos, and U. Schwingenschlögl, Appl. Phys. Rev. **2**, 021306 (2015); H. Wang, A. Chroneos, C. A. Londos, E. N. Sgourou, and U. Schwingenschlögl, Sci. Rep. **4**, 4909 (2014); H. Wang, A. Chroneos, C. A. Londos, E. N. Sgourou, and U. Schwingenschlögl, Appl. Phys. Lett. **103**, 052101 (2013).
[37]R. Kube, H. Bracht, A. Chroneos, M. Posselt, and B. Schmidt, J. Appl. Phys. **106**, 063534 (2009); G. Impellizzeri, S. Boninelli, F. Priolo, E. Napolitani, C. Spinella, A. Chroneos, and H. Bracht, *ibid.* **109**, 113527 (2011).
[38]R. Kube, H. Bracht, J. L. Hansen, A. N. Larsen, E. E. Haller, S. Paul, and W. Lerch, J. Appl. Phys. **107**, 073520 (2010); C. A. Londos, N. Sarlis, L. G. Fytros, and K. Papastergiou, Phys. Rev. B **53**, 6900 (1996); N. Sarlis, C. A. Londos, and L. Fytros, J. Appl. Phys. **81**, 1645 (1997).
[39]A. Chroneos and H. Bracht, Appl. Phys. Rev. **1**, 011301 (2014); A. Chroneos, H. Bracht, R. W. Grimes, and B. P. Uberuaga, Appl. Phys. Lett. **92**, 172103 (2008); H. Bracht, T. Sudkamp, M. Radek, and A. Chroneos, Appl. Phys. Rev. **2**, 036102 (2015).
[40]V. Saltas, A. Chroneos, and F. Vallianatos, Mater. Chem. Phys. **181**, 204 (2016).
[41]H. Bracht, E. E. Haller, and R. Clark-Phelps, Phys. Rev. Lett. **81**, 393 (1998).
[42]H. Bracht, Physica B **376–377**, 11 (2006).
[43]R. Kube, H. Bracht, E. Hüger, H. Schmidt, J. L. Hansen, A. N. Larsen, J. W. Ager III, E. E. Haller, T. Geue, and J. Stahn, Phys. Rev. B **88**, 085206 (2013).
[44]Y. Okada and Y. Tokumaru, J. Appl. Phys. **56**, 314 (1984).
[45]S. Rajagopalan, IL Nuovo Cimento **51**, 222 (1979).
[46]D. S. Kim, H. L. Smith, J. L. Niedziela, C. W. Li, D. L. Abernathy, and B. Fultz, Phys. Rev. B **91**, 014307 (2015).
[47]M. Werner, H. Mehrer, and H. D. Hochheimer, Phys. Rev. B **32**, 3930 (1985).
[48]N. A. Stolwijk, W. Frank, J. Hölzl, S. J. Pearton, and E. E. Haller, J. Appl. Phys. **57**, 5211 (1985).
[49]H. Bracht, N. A. Stolwijk, and E. Mehrer, Phys. Rev. B **43**, 14465 (1991).
[50]H. Bracht, Mater. Sci. Semicond. Process. **7**, 113 (2004).
[51]E. Hüger, U. Tietze, D. Lott, H. Bracht, D. Bougeard, E. E. Haller, and H. Schmidt, Appl. Phys. Lett. **93**, 162104 (2008).
[52]H. M. Kagaya, N. Shoji, and T. Soma, Phys. Status Solidi B **139**, 417 (1987).
[53]R. Krishman, R. Srinivasan, and S. Deverayanan, in *Thermal Expansion of Crystals* (Pergamon Press, Oxford, 1979).
[54]A. Di Cicco, A. C. Frasini, M. Minicucci, E. Principi, J.-P. Itiè, and P. Munsch, Phys. Status Solidi **240**, 19 (2003).
[55]C. Claeys and E. Simoen, *Germanium-Based Technologies: From Materials to Devices* (Elsevier, 2007); A. Chroneos, J. Appl. Phys. **105**, 056101 (2009); H. Tahini, A. Chroneos, R. W. Grimes, U. Schwingenschlögl, and A. Dimoulas, J. Phys.: Condens. Matter **24**, 195802 (2012); A. Chroneos, J. Appl. Phys. **107**, 076102 (2010).
[56]S. Brotzmann and H. Bracht, J. Appl. Phys. **103**, 033508 (2008).
[57]S. Brotzmann, H. Bracht, J. Lundsgaard Hansen, A. Nylandsted Larsen, E. Simoen, E. E. Haller, J. S. Christensen, and P. Werner, Phys. Rev. B **77**, 235207 (2008).
[58]A. Chroneos, R. W. Grimes, B. P. Uberuaga, and H. Bracht, Phys. Rev. B **77**, 235208 (2008).
[59]H. Tahini, A. Chroneos, R. W. Grimes, U. Schwingenschlögl, and H. Bracht, Appl. Phys. Lett. **99**, 072112 (2011).
[60]A. Chroneos and R. V. Vovk, J. Mater. Sci.: Mater. Electron. **26**, 2113 (2015).
[61]A. Chroneos and R. V. Vovk, Mater. Res. Express **2**, 036301 (2015).
[62]A. Chroneos, Y. Panayiotatos, and R. V. Vovk, J. Mater. Sci.: Mater. Electron. **26**, 2693 (2015).
[63]A. Chroneos and R. V. Vovk, J. Mater. Sci.: Mater. Electron. **26**, 3787 (2015).
[64]A. Chroneos and R. V. Vovk, J. Mater. Sci.: Mater. Electron. **26**, 7378 (2015).
[65]P. Dorner, W. Gust, A. Lodding, H. Odelius, B. Predel, and U. Roll, Acta Metall. **30**, 941 (1982).
[66]G. Vogel, G. Heffich, and H. Mehrer, J. Phys. C: Solid State Phys. **16**, 6197 (1983).
[67]H. H. Silvestri, H. Bracht, J. L. Hansen, A. N. Larsen, and E. E. Haller, Semicond. Sci. Technol. **21**, 758 (2006).
[68]P. Dorner, W. Gust, A. Lodding, H. Odelius, B. Predel, and U. Roll, Z. Metallkd. **73**, 325 (1982).
[69]H. Y. Liu, W. Z. Sun, Q. Y. Hao, H. Y. Wang, and C. C. Liu, J. Alloys Compd. **475**, 923 (2009).
[70]J. L. Roehl, A. Kolagatla, V. K. K. Gangur, S. V. Khare, and R. J. Phaneuf, Phys. Rev. B **82**, 165335 (2010).
[71]S. T. Murphy, A. Chroneos, C. Jiang, U. Schwingenschlögl, and R. W. Grimes, Phys. Rev. B **82**, 073201 (2010).
[72]J. A. del Alamo, Nature **479**, 317 (2011).
[73]J. L. Rohl, S. Aravelli, S. V. Khare, and R. J. Phaneuf, Surf. Sci. **606**, 1303 (2012).
[74]H. P. Komsa and A. Pasquarello, J. Phys.: Condens. Matter **24**, 045801 (2012).
[75]S. Adachi, *Physical Properties of III–V Semiconductor Compounds* (Wiley, 1992).
[76]L. Wang., L. Hsu, E. E. Haller, J. W. Erickson, A. Fischer, K. Eberl, and M. Cardona, Phys. Rev. Lett. **76**, 2342 (1996).
[77]E. F. Schubert, J. B. Stark, T. H. Chiu, and B. Tell, Appl. Phys. Lett. **53**, 293 (1988); E. F. Schubert, J. M. Kuo, R. F. Kopf, H. S. Luftman, L. C. Hopkins, and N. J. Sauer, J. Appl. Phys. **67**, 1969 (1990).
[78]J. F. Wager, J. Appl. Phys. **69**, 3022 (1991).
[79]S. Yu, T. Y. Tan, and U. Gösele, J. Appl. Phys. **69**, 3547 (1991); T. Y. Tan, H. M. You, U. M. Gösele, W. Jäger, D. W. Boeringer, F. Zypman, R. Tsu, and S. T. Lee, *ibid.* **72**, 5206 (1992).
[80]H. A. Tahini, A. Chroneos, S. T. Murphy, U. Schwingenschlögl, and R. W. Grimes, J. Appl. Phys. **114**, 063517 (2013).
[81]M. P. Chase, M. D. Deal, and J. D. Plummer, J. Appl. Phys. **81**, 1670 (1997).
[82]R. Mosca, P. Bussei, S. Franchi, P. Frigeri, E. Gombia, A. Carnera, and M. Peroni, J. Appl. Phys. **93**, 9709 (2003).
[83]M. Gonzalez Debs and T. F. Kuech, J. Appl. Phys. **99**, 123710 (2006).
[84]R. E. Goacher, S. Hedge, H. Luo, and J. A. Gardella, Jr., J. Appl. Phys. **106**, 044302 (2009).
[85]V. Saltas, A. Chroneos, and F. Vallianatos, RSC Adv. **6**, 53324 (2016).
[86]E. M. Omelyanovskii, A. V. Pakhomov, A. J. Polyakov, A. V. Govorkov, O. M. Borodina, and A. S. Bruk, Sov. Phys.—Semicond. **22**, 763 (1988).
[87]J. Ohsawa, H. Kakinoki, H. Ikeda, and M. Migitaka, J. Electrochem. Soc. **137**, 2608 (1990).
[88]S. S. Khludkov, O. B. Koretskaya, and G. R. Burnashova, Semiconductors **40**, 999 (2006).
[89]J. S. Blakemore, J. Appl. Phys. **53**, R123 (1982).
[90]M. Baublitz, Jr. and A. L. Ruoff, J. Appl. Phys. **53**, 6179 (1982); J. M. Besso, J. P. Itié, A. Polian, and G. Weill, Phys. Rev. B **44**, 4214 (1991); J. Wang, B. Wu, G. Zhang, L. Tian, G. Gu, and C. Gao, RSC Adv. **6**, 10144 (2016).
[91]F. Vallianatos and K. Eftaxias, Phys. Earth Planet. Inter. **71**, 141 (1992).
[92]H. J. McSkimin, A. Jayaraman, and P. Andreatch, Jr., J. Appl. Phys. **38**, 2362 (1967).

[93]H. Mehrer, *Diffusion in Solids* (Spinger, 2007).
[94]M. Kazimi, Am. Sci. **91**, 408 (2003).
[95]W. E. Lee, M. Gilbert, S. T. Murphy, and R. W. Grimes, J. Am. Ceram. Soc. **96**, 2005 (2013).
[96]M. Lung and O. Gremm, Nucl. Eng. Des. **180**, 133 (1998).
[97]M. Stan, Mater. Today **12**, 20 (2009).
[98]R. W. Grimes and C. R. A. Catlow, Proc. R. Soc. London A **335**, 609 (1991).
[99]K. Govers, S. Lemehov, M. Hou, and M. Verwerft, J. Nucl. Mater. **366**, 161 (2007).
[100]A. Chroneos, M. J. D. Rushton, C. Jiang, and L. H. Tsoukalas, J. Nucl. Mater. **441**, 29 (2013).
[101]K. E. Sickafus, R. W. Grimes, J. A. Valdez, A. Cleave, M. Tang, M. Ishimaru, S. M. Corish, C. R. Stanek, and B. P. Uberuaga, Nat. Mater. **6**, 217 (2007).
[102]T. Ichinomiya, B. P. Uberuaga, K. E. Sickafus, Y. Nishiura, M. Itakura, Y. Chen, Y. Kaneta, and M. Kinoshita, J. Nucl. Mater. **384**, 315 (2009).
[103]M. Bertolus, M. Freyss, B. Dorado, G. Martin, K. Hoang, S. Maillard *et al.*, J. Nucl. Mater. **462**, 475 (2015).
[104]N. V. Sarlis and E. S. Skordas, Solid State Ionics **290**, 121 (2016).
[105]M. W. D. Cooper, M. J. D. Rushton, and R. W. Grimes, J. Phys.: Condens. Matter **26**, 105401 (2014).
[106]M. W. D. Cooper, S. T. Murphy, P. C. M. Fossati, M. J. D. Rushton, and R. W. Grimes, Proc. R. Soc. London A **470**, 20140427 (2014).
[107]M. J. D. Rushton and A. Chroneos, Sci. Rep. **4**, 6068 (2014).
[108]M. W. D. Cooper, S. T. Murphy, M. J. D. Rushton, and R. W. Grimes, J. Nucl. Mater. **461**, 206 (2015).
[109]M. W. D. Cooper, M. E. Fitzpatrick, L. H. Tsoukalas, and A. Chroneos, Mater. Res. Express **3**, 065501 (2016).
[110]D. C. Parfitt, M. W. D. Cooper, M. J. D. Rushton, S.-R. G. Christopoulos, M. E. Fitzpatrick, and A. Chroneos, RSC Adv. **6**, 74018 (2016).
[111]P. Vinet, J. R. Smith, J. Ferrante, and J. H. Rose, Phys. Rev. B. **35**, 1945 (1987).
[112]J. H. Rose, J. R. Smith, F. Guinea, and J. Ferrante, Phys. Rev. B. **29**, 2963 (1984).
[113]M. S. Anderson and C. A. Swenson, Phys. Rev. B **31**, 668 (1985).
[114]G. Dolling, R. A. Cowley, and A. D. B. Woods, Can. J. Phys. **43**, 1397 (1965).
[115]I. J. Fritz, J. Appl. Phys. **47**, 4353 (1976).
[116]F. D. Murnaghan, Proc. Natl. Acad. Sci. U. S. A. **30**, 244 (1944).
[117]F. Birch, Phys. Rev. **71**, 809 (1947).
[118]K. Levenberg, Q. Appl. Math. **2**, 164 (1944).
[119]D. Marquardt, SIAM J. Appl. Math. **11**, 431 (1963).
[120]A. K. Sengupta, J. Banerjee, R. K. Bhagat, R. Ramachandran, S. Majumdar, and R. Division, "Thermal expansion data of (Th,U)O_2 fuels," Report No. BARC/2000/E/008, 2000.
[121]H. Bracht, S. P. Nicols, W. Walukiewicz, J. P. Silveira, F. Briones, and E. E. Haller, Nature (London) **408**, 69 (2000).
[122]H. Bracht, S. P. Nicols, E. E. Haller, J. P. Silveira, and F. Briones, J. Appl. Phys. **89**, 5393 (2001).
[123]H. A. Tahini, A. Chroneos, H. Bracht, S. T. Murphy, R. W. Grimes, and U. Schwingenschlögl, Appl. Phys. Lett. **103**, 142107 (2013).
[124]A. V. G. Chizmeshya, M. R. Bauer, and J. Kouvetakis, Chem. Mater. **15**, 2511 (2003).
[125]R. Roucka, J. Tolle, C. Cook, A. V. G. Chizmeshya, J. Kouvetakis, V. D'Costa, J. Menendez, and Z. D. Chen, Appl. Phys. Lett. **86**, 191912 (2005).
[126]J. Kouvetakis, J. Menendez, and A. V. G. Chizmeshya, Ann. Rev. Mater. Res. **36**, 497 (2006).
[127]A. Chroneos, H. Bracht, R. W. Grimes, and B. P. Uberuaga, Mater. Sci. Eng. B **154–155**, 72 (2008).
[128]A. Chroneos, H. Bracht, C. Jiang, B. P. Uberuaga, and R. W. Grimes, Phys. Rev. B **78**, 195201 (2008).
[129]A. Chroneos, C. Jiang, R. W. Grimes, U. Schwingenschlögl, and H. Bracht, Appl. Phys. Lett. **94**, 252104 (2009).
[130]A. Chroneos, C. Jiang, R. W. Grimes, U. Schwingenschlögl, and H. Bracht, Appl. Phys. Lett. **95**, 112101 (2009).
[131]S. T. Murphy, E. E. Jay, and R. W. Grimes, J. Nucl. Mater. **447**, 143 (2014).
[132]D. C. Parfitt, C. L. Bishop, M. R. Wenman, and R. W. Grimes, J. Phys. Condens. Matter **22**, 175004 (2010).
[133]B. Dorado, B. Amadon, M. Freyss, and M. Bertolus, Phys. Rev. B **79**, 235125 (2009).
[134]B. Dorado, M. Freyss, B. Amadon, M. Bertolus, G. Jomard, and P. Garcia, J. Phys. Condens. Matter **25**, 333201 (2013).
[135]E. Vathonne, J. Wiktor, M. Freyss, G. Jomard, and M. Bertolus, J. Phys. Condens. Matter **26**, 325501 (2014).
[136]D. Rupasov, A. Chroneos, D. Parfitt, J. A. Kilner, R. W. Grimes, S. Ya. Istomin, and E. V. Antipov, Phys. Rev. B **79**, 172102 (2009).
[137]T. J. Pennycook, M. J. Beck, K. Varga, M. Varela, S. J. Pennycook, and S. T. Pantelides, Phys. Rev. Lett. **104**, 115901 (2010).
[138]A. Kushima and B. Yildiz, J. Mater. Chem. **20**, 4809 (2010).
[139]I. D. Seymour, A. Chroneos, J. A. Kilner, and R. W. Grimes, Phys. Chem. Chem. Phys. **13**, 15305 (2011).
[140]I. D. Seymour, A. Tarancon, A. Chroneos, D. Parfitt, J. A. Kilner, and R. W. Grimes, Solid State Ionics **216**, 41 (2012).